Antiviral Research 161 (2019) 144–153

Contents lists available at ScienceDirect

Antiviral Research

journal homepage: www.elsevier.com/locate/antiviral

IgA targeting on the α-molecular recognition element (α-MoRE) of viral phosphoprotein inhibits measles virus replication by interrupting formation and function of P-N complex intracellularly

Dihan Zhou[a,b,1], Yi Yang[a,c,1], Bali Zhao[a,c], Jie Yu[a,c], Yuan Cao[a,c], Hu Yan[a,c], Wei Zhao[a,c], Longyun Chen[d], Fang Chen[b], Xiaodan Li[b], Ejuan Zhang[a], Jingyi Yang[a], Maohua Zhong[a], Mingzhou Chen[d], Qinxue Hu[a], Li Deng[b,**], Huimin Yan[a,*]

[a] Mucosal Immunity Research Group, State Key Laboratory of Virology, Wuhan Institute of Virology, Chinese Academy of Sciences, Wuhan, Hubei, 430071, China
[b] Guangzhou Institute of Pediatrics, Guangzhou Women and Children Medical Center, Guangzhou, 510623, China
[c] University of Chinese Academy of Sciences, Beijing, 100049, China
[d] State Key Laboratory of Virology and Modern Virology Research Center, College of Life Sciences, Wuhan University, Wuhan, 430072, China

ARTICLE INFO

Keywords:
IgA
Measles virus
Viral phosphoprotein
α-Molecular recognition element
Intracellular neutralization
P-N complex

ABSTRACT

Secretory IgA (SIgA) antibody is unique for its capability to transit through epithelial cells by transcytosis and thus has opportunities and probabilities to interact with all viral components during viral replication which may result in the inhibition of viral replication intracellularly. Here, we report a novel IgA mAb 1D11-IgA against phosphoprotein (P) of measles virus (MV), which is able to interact specifically with P in MV infected Vero-pIgR cells grown in a two-chamber transwell system. The binding epitope of 1D11-IgA involves a key residue proline 23 in P protein, which is among the α-molecular recognition element (α-MoRE) of P and critical for N^0-P complex. The antibody appears to block P to interact with N in P-N complex and thus may inhibit the function of viral RdRp complex, which results in decreased synthesis of viral genome RNA and mRNA. Our data together demonstrate that IgA is able to interact with viral phosphoprotein intraepithelial cells and neutralize viral replication by interrupting formation of P-N complex and function of RdRp. The findings highlight that IgA has a unique anti-viral activity by targeting viral conserved components critical for viral replication, which serves as a proof-of-concept assessment of the druggability of mononegavirales P-N interfaces.

1. Introduction

Immunoglobulin A (IgA), as the predominant antibody produced in mucosal areas, provides the very initial immunologic barriers against various pathogens (Lamm, 1997; Mazanec et al., 1993). A number of studies documented that secretory IgA (SIgA) plays key roles in mucosal protection constantly against virus infection in different anatomic locations related to mucosal epithelial cells through several proposed mechanisms (Corthesy, 2013). These include blocking infection at the apical surface ('immune exclusion'), neutralizing virus intracellularly ('intracellular neutralization'), and excreting virus across epithelial cells ('antigen excretion') (Strugnell and Wijburg, 2010). Intracellular neutralization occurs when SIgA intersects from the basolateral surface of epithelial cells and interacts with viruses (Mazanec et al., 1992). In this regard, a virus specific SIgA has intra-epithelial immune activities and can inhibit viral intracellular replication at very early stages (Mazanec et al., 1995).

Specific SIgA antibody can conceivably contact the antigens of a virus that is infecting the same cell due to its mandatory transepithelial route to the secretions (Mantis et al., 2011). Effects and mechanisms for the intracellular interactions between a specific SIgA antibody and the viral components would be determined by the transcytotic pathway of the IgA, its specificity for particular viral components, and the life cycle of the individual virus inside a mucosal epithelial cell. It is known that IgA antibodies against different categories of viral antigens have different anti-viral efficiencies (Yan et al., 2002; Zhou et al., 2011). For instance, studies with specific SIgA antibodies against internal viral proteins such as the VP6 protein of rotavirus (Burns et al., 1996;

* Corresponding author.
** Corresponding author.
E-mail addresses: drdengli@126.com (L. Deng), hmyan@wh.iov.cn (H. Yan).
[1] These authors contributed equally to the work.

https://doi.org/10.1016/j.antiviral.2018.11.014
Received 24 June 2018; Received in revised form 25 November 2018; Accepted 26 November 2018
Available online 28 November 2018
0166-3542/

Corthesy et al., 2006) and the matrix protein (M) of measles virus (MV) revealed that the IgA antibodies are indeed able to bind to both newly synthesized viral surface and internal antigens inside a cell during viral replication through polymeric immunoglobulin receptor (pIgR)-mediated transcytosis, and such IgAs proactively participate in mucosal immune protection via intracellular neutralization (Burns et al., 1996). The intracellular antiviral activities of an IgA antibody could be speculated based upon the type of viral component, the active epitope, the characteristic of a particular virus lifecycle, and the opportunities for a transcytosing IgA antibody to meet its prospective target, however, how the IgA antibody interact with its prospective target inside cells and the exact molecular mechanisms of this intracellular interaction between a virus and an IgA antibody remain to be determined.

In the present study, we generated a panel of IgG monoclonal antibodies (mAbs) against phosphoprotein (P) of MV and successfully obtained two clones of IgA mAb specifically against different epitopes of P. By employing polarized epithelial cells grown in a two-chamber transwell system, we investigated the interaction between IgA antibody and viral phosphoprotein inside MV infected epithelial cells for further understanding the molecular mechanism as to how P-specific IgA inhibits MV replication intracellularly. We found a monoclonal antibody 1D11-IgA targeting on the α-molecular recognition element (α-MoRE) of viral P blocks the complex formation of P with a soluble, monomeric form of nucleoprotein N and thus inhibiting RNA replication and mRNA expression of the viral genome.

2. Materials and methods

2.1. Cells and virus

Vero C1008 (ATCC CRL 1587) and Caco-2 (ATCC HTB-37) cells were obtained from ATCC. Vero-pIgR cell line was generated by stably expressing pIgR in Vero cells (Huang et al., 1999; Yan et al., 2002). Both cell lines were cultured in DMEM medium contained 10% fetal bovine serum, penicillin and streptomycin at 37 °C. SP2/0 (ATCC CRL 1581) and hybridomas were cultured in RPMI-1640 medium contained 10% fetal bovine serum, penicillin and streptomycin at 37 °C. The Edmonston strain of MV (ATCC VR-24) was propagated in Vero cells.

2.2. Mice

6–8 weeks old male BALB/c mice were obtained from Beijing Vital River Laboratory Animal Technology, China, and all animal experiments were performed according to Regulations for the Administration of Affairs Concerning Experimental Animals in China (1988).

2.3. Hybridomas

The full length P protein of MV Edmonston strain (GenBank accession no. AAF85692.1) expressed in *E.* coli was used as the antigen to immunize BALB/c mice, and MV P specific B cells were collected. Fusion of MV P specific B cells with SP2/0 cells was performed as described elsewhere (Kohler and Milstein, 1975). Thereafter, a panel of murine IgG secreting monoclonal hybridomas against MV P were obtained, including 1D11-IgG, 7F1-IgG, 7G4-IgG and 8C4-IgG. Two IgA secreting monoclonal hybridomas, 1D11-IgA and 7F1-IgA, were obtained by repeated cycles of limiting dilution and spontaneous isotype switch. Two corresponding pairs of murine anti-hemagglutinin IgA/IgG antibodies (16CD11-IgA and 16CD11-IgG) and anti-matrix protein IgA/IgG antibodies (5H7-IgA and 5H7-IgG) were described previously (Zhou et al., 2011). One IgA monoclonal antibody (mAb) against HIV gp120 was used as the irrelevant IgA control (a gift from Y. T. Huang at Case Western Reserve University, OH).

2.4. IgA transcytosis in a transwell system

Vero-pIgR cells were cultured in 0.4-μm-pore-size Transwells (Costar, REF3460), in which 1×10^5 cells were seeded and cultured in each chamber 4 days. Transcytosis of antibodies from the basolateral to the apical surfaces of epithelial cells was assessed by addition of 20 μg mAbs in 120 μl medium into each basal chamber, and collection of the apical supernatants at 0, 12, 24, 36, and 48 h for ELISA assay (Yan et al., 2002).

2.5. Immunofluorescent staining and confocal microscopy

Polarized Vero-pIgR cell monolayers were grown in Transwells and infected with MV at an MOI of 1 as previously described (Zhou et al., 2011). Membrane-attached cells were fixed and permeabilized by 4% paraformaldehyde and 0.1% Triton X-100 in PBS (pH 7.4). DAPI was used to stain the nuclei of the cells. Fluorescein isothiocyanate (FITC)-conjugated goat anti-mouse IgA (Southern Biotechnology) was used to detect IgA antibodies. Anti-P 7G4-IgG mAb was used to detect MV P protein, while Alexa Fluor (R) 555 goat anti-mouse IgG (Invitrogen) was used as a secondary antibody to detect anti-P 7G4-IgG mAb.

2.6. Traditional virus neutralization assay

100 PFU of MV virions per well in 120 μl medium were mixed with either 40 μg of mAbs in 120 μl medium or 120 μl medium alone, and incubated at 37 °C for 2 h. The mixtures were used to infect Vero cells in 24-well plates. 2 h after infection, the cells were washed by fresh medium for three times and virus titers were assayed by plaque assay.

2.7. Intracellular virus neutralization assay

The two-chamber transwell system seeded with Vero-pIgR, Vero or Caco-2 cells was set up as described above. Monolayer cells were infected with MV at an MOI of 1 for two hours and washed by fresh medium for three times. 20 μg of mAbs in 120 μl medium was added into the basal chambers with medium alone being used as the negative control. Cell lysates were collected at 48 h after initial exposure to the virus. Virus titers were quantified by a plaque assay as described previously (Yan et al., 2002).

2.8. Co-immunoprecipitation and western blotting

The truncated and mutated clones of P protein were constructed into pET30a plasmid (Novagen cat no.69909-3) for recombinant protein preparation and binding site mapping. The MV-P and MV-N full length clones were constructed into pcDNA3.1 plasmid (Invitrogen) for transfection and co-immunoprecipitation assay. Briefly, 2×10^5 Vero-pIgR cells were seeded and cultured in Transwells (Costar, REF3460) for 1 day, and then transfected with 1.5 μg of the plasmid by lipofectamine 3000 (Thermo Fisher Scientific). 20 μg of anti-P IgA or control IgA in 120 μl DMEM was added to the basal chamber. Cells were collected 48 h after transfection and lysed with TBS buffer plus 1% triton-100 and 0.2% protease inhibitor mixture (Roche Molecular Biochemicals) for co-immunoprecipitation. Beads (Invitrogen) conjugated with anti-P 8C4-IgG antibody were used to immunoprecipitate MV P in cell lysates. Anti-P 7G4-IgG, anti-N 16CF7-IgG, and anti β-actin IgG (Beijing Ray antibody biotech) were used as the primary antibodies to detect MV P protein, N protein and β-actin, respectively, while goat anti mouse IgG-HRP (the Jackson immunoreaserch laboratories) was used as a secondary antibody.

2.9. Quantitative real-time PCR

The extraction of cell total RNA was performed by using Trizol (Sigma T9424). The cDNA was prepared from total RNA with a Thermo

Scientific Revert Aid First strand cDNA Synthesis Kit (Thermo Scientific) using random primers, followed by quantitative real-time PCR under the CFX Connect Real-Time system (Bio-RAD). The delta-delta CT values were calculated and presented over the irrelevant IgA control as 100%. The primers used for quantitative real-time PCR assay are present in Table 4.

2.10. Statistical analysis

Data were analyzed using GraphPad Prism software (www.graphpad.com). All of the statistical analyses were performed with one way anova or two way anova. P values < 0.05 were considered statistically significant.

3. Results

3.1. Monoclonal anti-P IgA antibodies transport across polarized epithelial cells via pIgR readily and specifically interact with viral P protein efficiently inside epithelial cells during MV infection

Measles virus (MV) was used as a model to investigate the functions of IgA antibodies in our previous studies (Yan et al., 2002; Zhou et al., 2011). By using this well-established model in our laboratory, here we investigated the intracellular interaction between IgA antibody and viral phosphoprotein. Two IgA antibodies against phosphoprotein were firstly tested for their transcytosis activities across polarized Vero-pIgR monolayers compared with their corresponding IgG antibodies. As shown in Fig. 1A, both 1D11-IgA and 7F1-IgA were readily transported across the Vero-pIgR monolayers from the basolateral to the apical compartments in a time dependent manner, and there was no difference in transport efficiency between these two IgA antibodies. In contrast, 1D11-IgG and 7F1-IgG showed no detectable transport in the Vero-pIgR monolayers. All antibodies showed no detectable transport in the polarized pIgR negative Vero monolayers (data not shown). These data indicated that the transcytosis of 1D11-IgA and 7F1-IgA was mediated by pIgR.

By using two-color immunofluorescent-staining assay and confocal microscopy, 1D11-IgA and 7F1-IgA antibodies were tested for their possible interactions with P protein in MV infected Vero-pIgR cells. As shown in Fig. 1B, 1D11-IgA and 7F1-IgA were observed in the cytoplasm of the uninfected cells either at 24 or 48 h after the addition of IgA, which is in accordance with the data of IgA transcytosis shown in Fig. 1A. Viral P protein could be observed in the cytoplasm of the infected cells both at 24 or 48 h.p.i., although more P protein was detected at 48 h.p.i. When anti-P IgA was applied in the MV infected cells, both 7F1-IgA and 1D11-IgA but not the irrelevant IgA were observed to be highly co-localized with P protein in the cytoplasm of cells. It is worth noting that the anti-P IgA antibodies accumulated significantly in the MV-infected cells compared to those in the uninfected cells, suggesting the interaction of IgA with newly synthesized viral P proteins.

Taken together, these results demonstrated that both monoclonal 1D11-IgA and 7F1-IgA antibodies transport across polarized epithelial cells via pIgR readily and specifically interact with newly synthesized P proteins during transcytosis in MV infected cells.

3.2. Despite having no traditional neutralization activity, 1D11-IgA inhibits MV replication in Vero-pIgR cells definitely via intracellular neutralization

It is believed that the anti-P antibodies unlikely neutralize infectious virus particles because P is an internal protein of MV. We firstly examined whether the monoclonal 1D11-IgG, 1D11-IgA, 7F1-IgG and 7F1-IgA antibodies could block the infection of MV by traditional neutralization. As expected, all of the four anti-P mAbs failed to cause any significant PFU reduction, as did the irrelevant IgA mAb and medium alone, while the anti-H mAb pair (16CD11-IgA and 16CD11-IgG) showed significant neutralization activity against MV similar to that as demonstrated in our previous study (Yan et al., 2002) (Table 1). These data together indicated that both anti-P IgA mAbs (1D11-IgA and 7F1-IgA) and IgG mAbs (1D11-IgG and 7F1-IgG) had no traditional neutralization activity against measles virus.

By using a two-chamber transwell model seeded with polarized Vero-pIgR cell monolayers, we subsequently investigated whether the anti-P IgA mAb has intracellular-neutralization activity. As shown in Table 2, 1D11-IgA reduced the virus titer by 69.7% compared with the control of medium alone ($P < 0.001$), whereas 1D11-IgG did not have such activity (0%). In addition, 7F1-IgA or 7F1-IgG treatment only resulted in marginal reduction of virus titer (3.95% and 1.12%, respectively), which were not statistically significant compared with the control of irrelevant IgA or medium alone (Table 2, Vero-pIgR). Furthermore, no significant viral reduction was observed for all the tested antibodies in Vero cells without pIgR (Table 2, Vero), further demonstrating that pIgR mediated the observed intracellular neutralization of 1D11-IgA.

When serially diluted 1D11-IgA and 1D11-IgG antibodies (0, 2.5, 5, 10, 20, and 40 μg per transwell), respectively, were tested for the intracellular neutralization activities in the same system as described above, 1D11-IgA showed the capacity to inhibit MV replication in a dose dependent manner in the range of 2.5–20 μg per transwell and reached saturation at the dose of 40 μg (Fig. 2A). In contrast, none of the tested 1D11-IgG doses showed inhibition effect on MV replication when the cells were infected with MV at an MOI of 1 (Fig. 2A). When the data was plotted as dose-response curve as Fig. 2B and compared with irrelevant IgA, 1D11-IgA showed typical dose-response in the concentration range of 2.5–20 μg and levelling off at 40 μg, while 1D11-IgG or irrelevant IgA showed no response at any concentration (Fig. 2B). Further compared to control with 20 μg irrelevant IgA or medium only, 1D11-IgA achieved similar and stable inhibition effects when the cells were infected with MV at an MOI of 0.1, 0.2 or 0.4 instead of at an MOI of 1 (Fig. 2C). Similar results were observed in Caco-2 cells (Fig. 2D). The data suggested that 1D11-IgA exerts antiviral activity inside viral infected cells and inhibits MV replication definitely via an intraepithelial mechanism.

3.3. The binding site of 1D11-IgA on P is located on the α-molecular recognition element (α-MoRE)

Given that both 1D11-IgA and 7F1-IgA antibodies can interact with P protein inside an MV infected cell, we next performed epitope mapping experiments to understand why only 1D11-IgA can inhibit MV replication intracellularly. To map the binding epitope of 1D11-IgA, twelve truncated P proteins and two full-length P proteins with a single mutation P_{E22A} and P_{P23A} were constructed and tested (Fig. 3A). After the first three round of 1D11-IgA epitope mapping assay, the binding site of 1D11-IgA likely locates within aa17-aa23 of MV P. Of note, PD10, PD11, PD12 but not PD09 could be detected by 1D11-IgA, indicating that the proline at aa23 of MV P is likely to be a key residue involved in 1D11-IgA binding. To confirm this, two point mutants of P proteins, P_{E22A} and $P_{P23A,}$ were generated and further assessed, showing that P_{E22A} but not P_{P23A} could be recognized by 1D11-IgA (Fig. 3A). On the other hand, only the peptide PW03 and PW04 which containing the proline at aa23 of MV P but not PW01 and PW02 could be bound by 1D11-IgA (Fig. 3B). The data further confirmed that P23 in MV P is a key residue involved in the binding of 1D11-IgA.

To map the epitope of 7F1-IgA (Fig. 3C), similar strategy was employed by using the eight truncated P proteins (PD1, PD2, PD3, PD4, PD5, PD6, PD13 and PD14) which were confirmed by western blotting in parallel with anti-His tag antibody (Fig. 3E). The binding site of 7F1-IgA was located within aa77-aa86 by comparing the results of PD6 and PD14 (Fig. 3C). To determine the critical amino acid residue(s) in the binding site of 7F1-IgA, 11-mer peptides containing point alanine substitution on each amino acid of aa77-aa86 were used for residue screening by ELISA. As shown in Fig. 3D, substitution of glycine at aa80

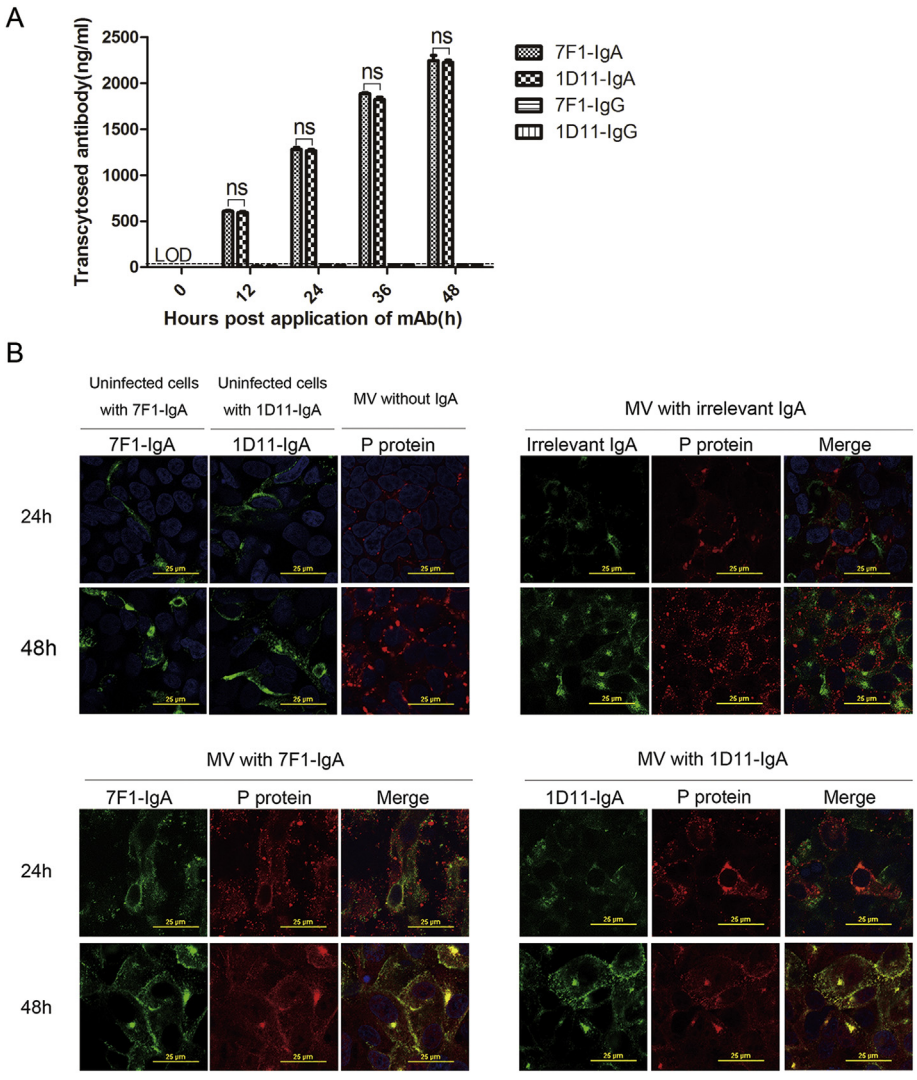

Fig. 1. (A) Transcytosis of anti-P IgA and IgG antibodies across polarized Vero-pIgR monolayers. The limit of detection (LOD) is 10 ng/ml by ELISA indicted by a dash line. **(B) Distribution of anti-P IgA antibodies in MV infected Vero-pIgR cells and their colocalization with MV P protein by confocal microscopy.** The polarized Vero-pIgR cell monolayers grown on polyester membranes were infected with measles virus at an MOI of 0.1 via the apical surfaces. 2 h later, 20 μg of 1D11-IgA, 7F1-IgA and irrelevant anti-HIV gp120 IgA mAbs were added to the basal chambers, respectively. At 24 h or 48 h after initial infection, the membrane-attached cells were fixed, permeabilized, and stained with Alexa Fluor (R) 555 goat-anti-mouse IgG to detect P protein and FITC-conjugated goat anti-mouse IgA to detect IgA antibodies. ns, $p \geq 0.05$.

Table 1
Neutralization activities of anti-P and anti-H IgA and IgG antibodies.[a]

mAb (166.7 μg/ml)	Virus titer (PFU/well)	%Reduction of virus titer[b]
Anti-P 1D11-IgA	32.5 ± 5.92[d]	8.45
Anti-P 1D11-IgG	34.60 ± 4.57[d]	2.53
Anti-P 7F1-IgA	37.3 ± 2.46[d]	0.00
Anti-P 7F1-IgG	34.50 ± 1.00[d]	2.82
Anti-H 16CD11-IgA	5.50 ± 2.86[c]	84.5
Anti-H 16CD11-IgG	7.00 ± 1.78[c]	80.3
Irrelevant IgA	32.60 ± 3.90[d]	8.17
Medium alone	35.50 ± 1.07	0.00

[a]Experiments were repeated at least twice with similar results. Results of a representative experiment are shown. Data are means ± SD ($n = 3$).
[b]Compared to medium alone.
[c,d] Statistical analyses were performed between medium alone negative control and each group; [c] indicates $P < 0.0001$ and [d] indicates $P \geq 0.05$ by unpaired one-way anova analysis.

(PT05), glutamine at aa81(PT06), or glutamic acid at aa85 with alanine (PT10) totally abolished the interaction between 7F1-IgA and the peptides, suggesting that G80, Q81 and E85 on MV P are essential for 7F1-IgA binding and that other residues like R77, I78, R79, G82, P83, and G84 are also likely to be involved.

In summary, the key binding site of 1D11-IgA includes a residue, or residues, within aa17-aa23 of MV P, while the key binding site of 7F1-IgA appears to include residues G80, Q81 and E85 in the PNT of P protein (Fig. 3F and G). The binding site of 1D11-IgA on P is among the α-molecular recognition element (α-MoRE), which is highly unstable but can bind with MV N^0 and be stabilized in N^0-P complex (Blocquel et al., 2014; Cevik et al., 2004; Guryanov et al., 2015; Johansson et al., 2003; Kingston et al., 2004). We also analyzed the N-terminal 38 amino acids of P by SWISS-MODEL, and obtained a typical 3D α-MoRE model (Fig. 3H) as same as reported by (Guryanov et al., 2015), in which the featured conserved hydrophobic amino acids (Table 3), such as Phe, Leu, Ile, and Val distributed evenly along the α-helix, and might provide a protein-protein hydrophobic interaction motif. These data together indicated that 1D11-IgA likely interferes with P to integrate into P-N complex.

3.4. Anti-P 1D11-IgA blocks interaction of P with N during MV replication

Based on the binding site of 1D11-IgA on P, which involves the conserved P23 in protein-protein hydrophobic interaction region of the PNT, we speculate that the formation of P-N complex and viral RNA synthesis might be interrupted by 1D11-IgA. To test this hypothesis, we performed immunoprecipitation assay to assess whether 1D11-IgA interferes with the interaction between P and N. As shown in Fig. 4A, N could be precipitated by P efficiently when medium alone or irrelevant IgA was used in the MV infected cells but only 13.5% of N protein was precipitated by P in the group of 1D11-IgA compared to that in the

Table 2
Intracellular neutralization of virus by anti-P IgA antibodies.[a]

Cell line	Vero –pIgR		Vero	
mAb (166.7 μg/ml)	Virus titer (PFU/well)	%Reduction of virus titer[b]	Virus titer (PFU/well)	%Reduction of virus titer[b]
Anti-P 1D11-IgA	2678.00 ± 248.06[c]	69.7	8670.00 ± 698.7[d]	3.02
Anti-P 1D11-IgG	8920.00 ± 289.82 [d]	0.00	8790.00 ± 234.94[d]	1.68
Anti-P 7F1-IgA	8500.00 ± 590.04[d]	3.95	8960.67 ± 374.89 [d]	0.00
Anti-P 7F1-IgG	8750.00 ± 292.13[d]	1.12	8879.33 ± 324.43[d]	0.68
Anti-M 5H7-IgA	1965.67 ± 291.35[c]	77.79	9346.67 ± 1133.1 [d]	0.00
Anti-M 5H7-IgG	8500.00 ± 624.52[d]	3.95	8956.00 ± 823.27 [d]	0.00
Irrelevant IgA	9050.00 ± 410.24 [d]	0.00	8845.00 ± 399.71[d]	1.06
Medium alone	8850.00 ± 728.62	0.00	8940.33 ± 252.30	0.00

[a]Experiments were repeated at least twice with similar results. Results of a representative experiment are shown. Data are means ± SD (n = 3).
[b]Compared to medium alone.
[c] and [d] Statistical analyses were performed between medium alone negative control and each group; [c] indicates $P < 0.001$ and [d] indicates $P \geq 0.05$ by two-way anova analysis.

group of medium alone. These results suggested that 1D11-IgA impairs the interaction between MV P and N.

To confirm the interaction between MV P, N and 1D11-IgA, expression plasmids encoding MV P and Flag-tagged N were constructed and assayed by co-transfection followed by treatment with or without anti-P IgA in basal chambers of the transwell model. As shown in Fig. 4B, an apparent association of P with N could be detected in the absence of any IgA or in the presence of 7F1-IgA or irrelevant IgA, but a significant impaired association of P with N was detected when 1D11-IgA was present in the chamber system seeded with Vero-pIgR cells. Only 31.5% of the N protein could be detected in the complex immunoprecipitated by P when 1D11-IgA used in the co-transfected cells compared to that with medium alone. Similar to the data shown in Fig. 4B, about 43% of the P protein could be detected in the complex immunoprecipitated by N when 1D11-IgA used in the co-transfected cells compared to that with medium alone (Fig. 4C). These results further confirmed that 1D11-IgA indeed interrupts the interaction between MV P and N protein, whereas 7F1-IgA does not interfere with the interaction between MV P and N protein.

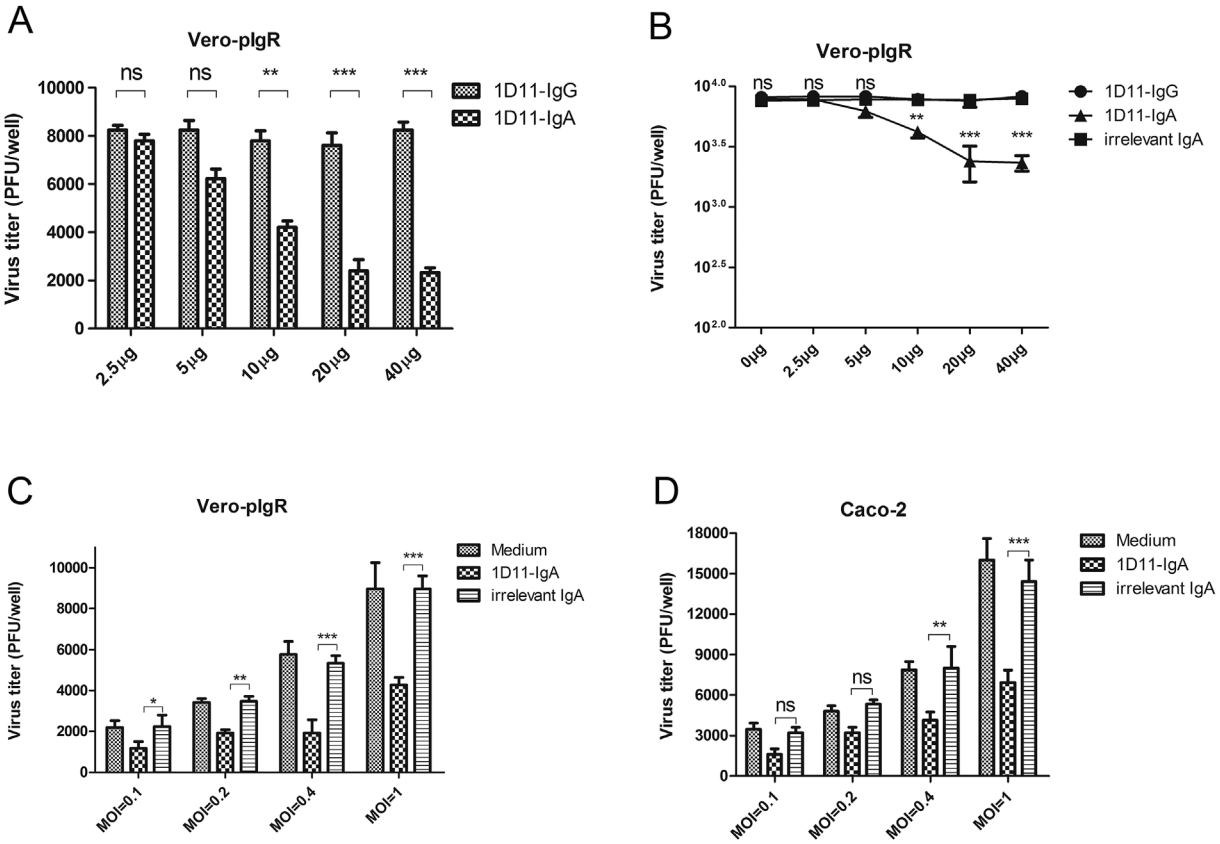

Fig. 2. Anti-P 1D11-IgA antibody inhibits MV replication in a dose-dependent manner. (A and B) Polarized Vero-pIgR cells grown in transwells were infected with measles virus at an MOI of 1. Then, 2 h.p.i., 2.5 μg, 5 μg, 10 μg, 20 μg or 40 μg of 1D11-IgA, 1D11-IgG or irrelevant IgA mAbs were added into the basal chambers. **(C)** Polarized Vero-pIgR cells or **(D)** Caco-2 cells grown in transwells were infected with measles virus at an MOI of 0.1, 0.2, 0.4 or 1, and 20 μg of 1D11-IgA, irrelevant IgA mAbs or medium as control were added into the basal chambers 2 h.p.i. Cell lysates were collected 48 h for Vero-pIgR cells **(A, B and C)** and 72 h for Caco-2 cells **(D)** after initial exposure to virus, and the virus titers were assessed by plaque assay. All the experiments were performed at least 3 times. ns, $p \geq 0.05$, *, $p < 0.05$, **, $p < 0.01$, ***, $p < 0.001$.

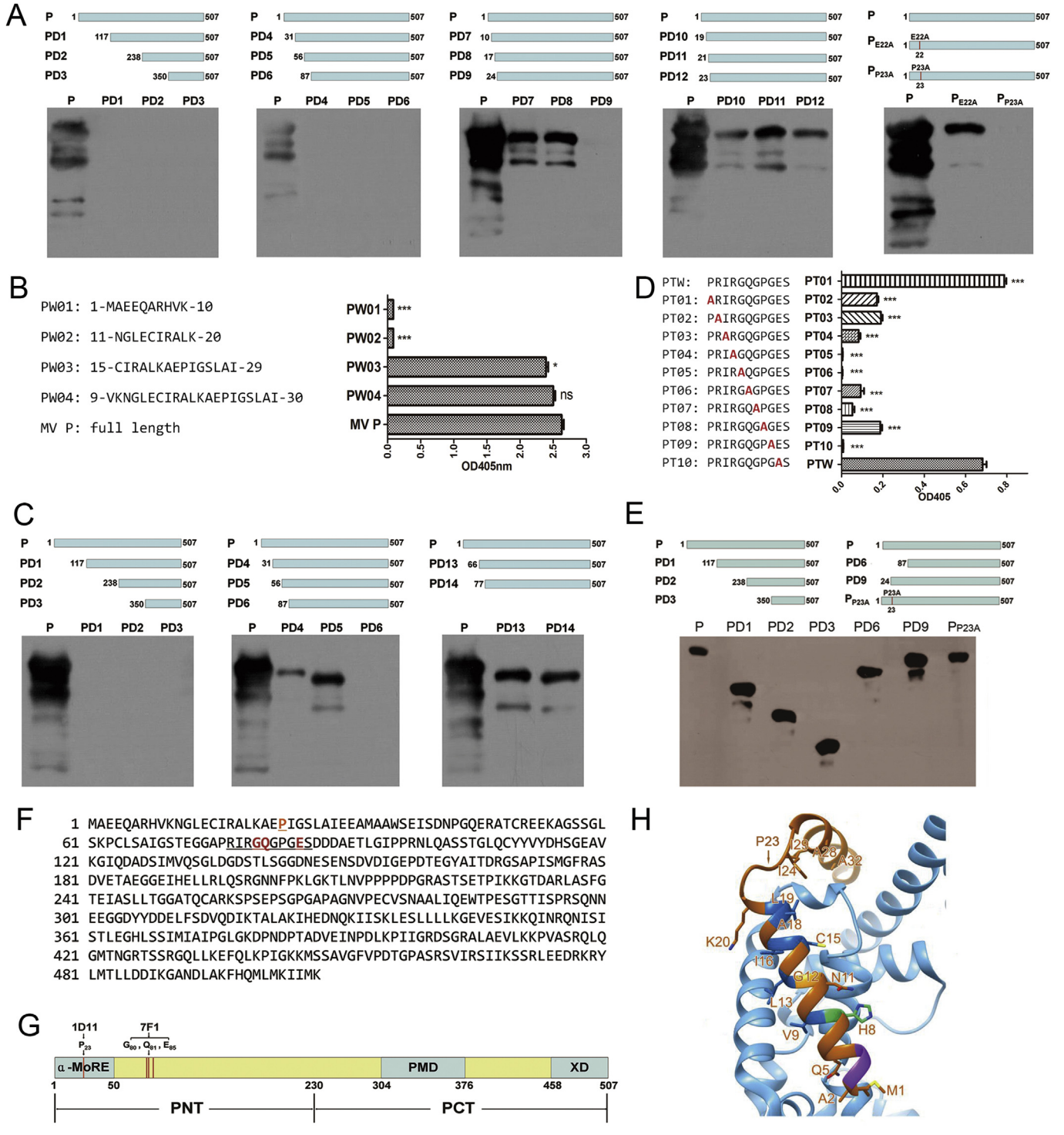

(caption on next page)

3.5. Anti-P 1D11-IgA exerts inhibitory effects on viral genomic RNA replication and viral mRNA synthesis

Considering that anti-P 1D11-IgA interrupts P to integrate into P-N complex and may interfere with the function of viral RdRp, we further tested the effects of 1D11-IgA on viral genome replication and viral gene expressions. To this regard, we quantified mRNAs of viral genes, viral genome and antigenome in MV infected Vero-pIgR cells by q-PCR. As shown in Fig. 5, the relative mRNA expression of viral genome RNA and antigenome RNA, viral N, P, M, and L genes, were compared alternatively between 1D11-IgA and irrelevant IgA based on double delta Ct analysis with the irrelevant IgA control as 100%. The expression of RNAs in the infected cells treated with 1D11-IgA decreased significantly. The negative-strand genome RNA, positive-strand full-length RNA (antigenome), mRNAs of N, P, M and L were reduced to 51%, 66%, 43%, 41%, 60%, and 37%, respectively, when 1D11-IgA was applied to MV infected cells compared to that of irrelevant IgA (Fig. 5). In parallel, the reproduced infectious viral particles detected by plaque assay were reduced significantly (Fig. 5) when 1D11-IgA was present compared with that treated with an irrelevant IgA. These results further

Fig. 3. Epitope mapping of 1D11-IgA and 7F1-IgA on P protein. (A) 12 N-terminal truncated P proteins (PD1, PD2, PD3, PD4, PD5, PD6, PD7, PD8, PD9, PD10, PD11, and PD12) and 2 full-length P proteins with a single mutation (P_{E22A} and P_{P23A}) were designed, expressed and assessed by western blotting using 1D11-IgA as the primary antibody.**(B)** Full-length MV P protein and peptides containing different sequences in aa1-aa30 of P protein and were assessed by ELISA using the peptides for coating and 1D11-IgA as the primary antibody. Optical density at 405 nm (OD 405 nm) was measured. Statistical analyses were performed between full length of P (positive control) and each peptide. ns, $p \geq 0.05$, *, $p < 0.05$, ***, $p < 0.001$. **(C)** N-terminal truncated P proteins (PD13 and PD14) were designed and expressed. PD13 and PD14 together with PD1, PD2, PD3, PD4, PD5, and PD6 were assessed by western blotting using 7F1-IgA as the primary antibody. **(D)** 11-mer peptides containing aa76-aa86 of P protein were alanine scanned and assessed by ELISA using the peptides for coating and 7F1-IgA as the primary antibody. Optical density at 405 nm (OD 405 nm) was measured. Statistical analyses were performed between PTW positive control and each mutated 11-mer peptide, **, $p < 0.01$, ***, $p < 0.001$. **(E)** N-terminal truncated P proteins (PD1, PD2, PD3, PD6, PD9) and a full-length P protein with a single mutation (P_{P23A}) were expressed and assessed by western blotting using mouse anti-His tag antibody as the primary antibody. **(F)** The key binding sites of 1D11-IgA and 7F1-IgA on P protein. P23 (labeled in orange) is necessary for the interaction between 1D11-IgA and P protein, while 7F1 interacts with a 10-amino-acid region (R77 to S86) on P protein, of which, 3 amino acids (G80, Q81 and E85 in red) are critical and the rest 7 amino acids play auxiliary roles. **(G)** Modular organization of P protein. The key binding site P23 of 1D11-IgA on P protein is labeled in orange and the key binding residues G80, Q81 and E85 of 7F1-IgA on P protein are labeled in red. **PNT**: N-terminal region of P; **PCT**: C-terminal region of P; **α-MoRE**: an α-helical conformation binding to N^0, also known as the N-terminal domain of P (P_{NTD}); **PMD**: P multimerization domain; **XD**: X domain binding to N_{TAIL}. **(H)** 3D model of N-terminal 38 amino acids of α-MoRE built by SWISS-MODEL and cartoon presented together with N showing the position of P23 on the P-N binding interface. The cartoon representation is modified from report by Sergey G. Guryanoy et al. (Guryanov et al., 2015), in which $P_{1\text{-}38}$ (orange-red) residues interacting with $N_{21\text{-}408}$ (sky blue) are shown. Colors represent residues conserved throughout the *Paramyxovirinae* as follows: violet, acidic; green, polar; blue, hydrophobic; and orange, glycine.

Table 3
Conservation of sequence around 1D11-IgA binding site.[a]

Species	Homologous sequence
Measles virus	VKNGLECIRALKAE**P**IGSLAI
Rinderpest virus	VNKGLECIKALRAR**P**LDPLVV
Dolphin morbillivirus	VNKGLECLKSLREN**P**PDAVEI
Peste-des-petits-ruminants virus	VNKGLECIKSLKAS**P**PDLSTI
Canine distemper virus	VNKGLECLKALREN**P**PDIEEI

[a] The P23 residues in MV P of morbilliviruses are highlighted in bold with underline. Conserved hydrophobic amino acids are underlined.

demonstrated that 1D11-IgA inhibits viral gene expression and viral genome replication, thus decreasing virus replication and production.

4. Discussion

The viral phosphoprotein (P), as an indispensable subunit of the viral polymerase complex, plays multiple roles in both viral transcription and replication (Bloyet et al., 2016; Bonetti et al., 2016; Bourhis et al., 2004, 2005, 2006; Brunel et al., 2014; Dosnon et al., 2015; Gruet et al., 2016; Karlin et al., 2002, 2003; Longhi et al., 2003; Noton and Fearns, 2015). More specifically, P is a viral internal structural component associated with large protein (L), nucleoprotein (N) and genome RNA of MV within viral particle. The formation of P-N complex is essential for viral gene expression and genome replication (Erales et al., 2015; Huber et al., 1991; Spehner et al., 1997), in which P is responsible for binding and delivery of N^0 to the newly synthesized genomic RNA (Buchholz et al., 1994; Ryan and Portner, 1990), and P-N complex is the substrate of nucleocapsid. Regarding the essential function of P in viral replication, it is conceivable that if there is an inhibitor specific against P could interact with P inside cell, the viral replication might be interfered efficiently. Based on this notion and the unique intracellular neutralization activity of IgA antibodies as demonstrated previously, we generated several IgA clones specific to different epitopes of P. This provided us the opportunity to examine IgA antibodies against MV internal protein P for the potential intracellular neutralization activity. Of interest, we found that only clone 1D11-IgA inhibited the replication of MV in Vero-pIgR cells used for the IgA function assay, whereas the 7F1-IgA clone did not have such activity, although it was able to transport through polarized cells and bound to P with a similar efficiency as that of 1D11-IgA.

The different antiviral activities showed between 1D11-IgA and 7F1-IgA inspired us to further explore the underlying mechanism. Therefore, we performed detailed epitope mapping for both 1D11-IgA and 7F1-IgA and found that the binding sites on P for 1D11-IgA and 7F1-IgA are indeed different. We found the P23 at the N-terminal of P protein is a key residue in the specific epitope involved in 1D11-IgA binding, and likely to be involved in mediating the interaction between P and N as evidenced by the immunoprecipitation results. Taken together, P23 is likely to be a cornerstone residue in P critical for the functionality of P-N complex and for viral genome replication. On the contrary, aa77-aa86 (RIRGQGPGES) on N-terminal moiety of P appears not to be involved in the interaction between P and N, though aa77-aa86 is essential for the binding of 7F1-IgA to P.

By further assessing the involvement of P23 in the α-molecular recognition element (α-MoRE) and its interaction with N^0 in N^0-P complex (Guryanov et al., 2015), it is revealed that P23 likely locates in the interface of P and N^0 as many structure analyses have suggested (Curran et al., 1995; Devasthanam, 2014; Kirchdoerfer et al., 2015; Lycke and Bemark, 2017). By comparing the sequence of MV phosphoprotein with those of several morbilliviruses retrieved from GenBank using BLAST, we also found that the proline residue (P23) in RALKAEP is very conserved among different morbillivirus species, while the hydrophobic amino acids distributed evenly along the α-helix sequence upstream and downstream of P23 are also conserved among these virus species (Table 3). Taking advantage of 1D11-IgA targeting the intrinsically disordered protein region (IDPR) in the intrinsically disordered protein (IDP) and its activity to interrupt the interaction of N^0–P_{NTD}, we speculate that P23 of N^0-P complex is a potential core target site for antiviral drugs.

Our study demonstrated for the first time that the MV

Table 4
Primer sequences used for RT-PCR.

Gene	Forward primer sequence (5′-3′)	Reverse primer sequence (3′-5′)
genome	ACCAAACAAAGTTGGGTAAGG	CTTAAAAGTGTGGCCATCTCGG
anti genome	ACCAGACAAAGCTGGGAATAG	CCAAAGAATGGTATAAGTTAGTCG
MV N	CACCGATGACCCTGACGTTAG	CACTACTAATCGGATCATCATGTG
MV P	CAATTGGATCAACTGAAGGCG	CACCGCTGTGATCATAAACAT
MV M	CTACGACTTCGACAAGTCGG	CAACAACCCCCAGCAGAAACAT
MV L	GGGATTCAGTTTACCCGAAAG	GGTCATGGAGGTAAGCTCCACT
β-actin	ATCATGAAGTGTGACGTGGACA	AGGAGCAATGATCTTGATCTTCA

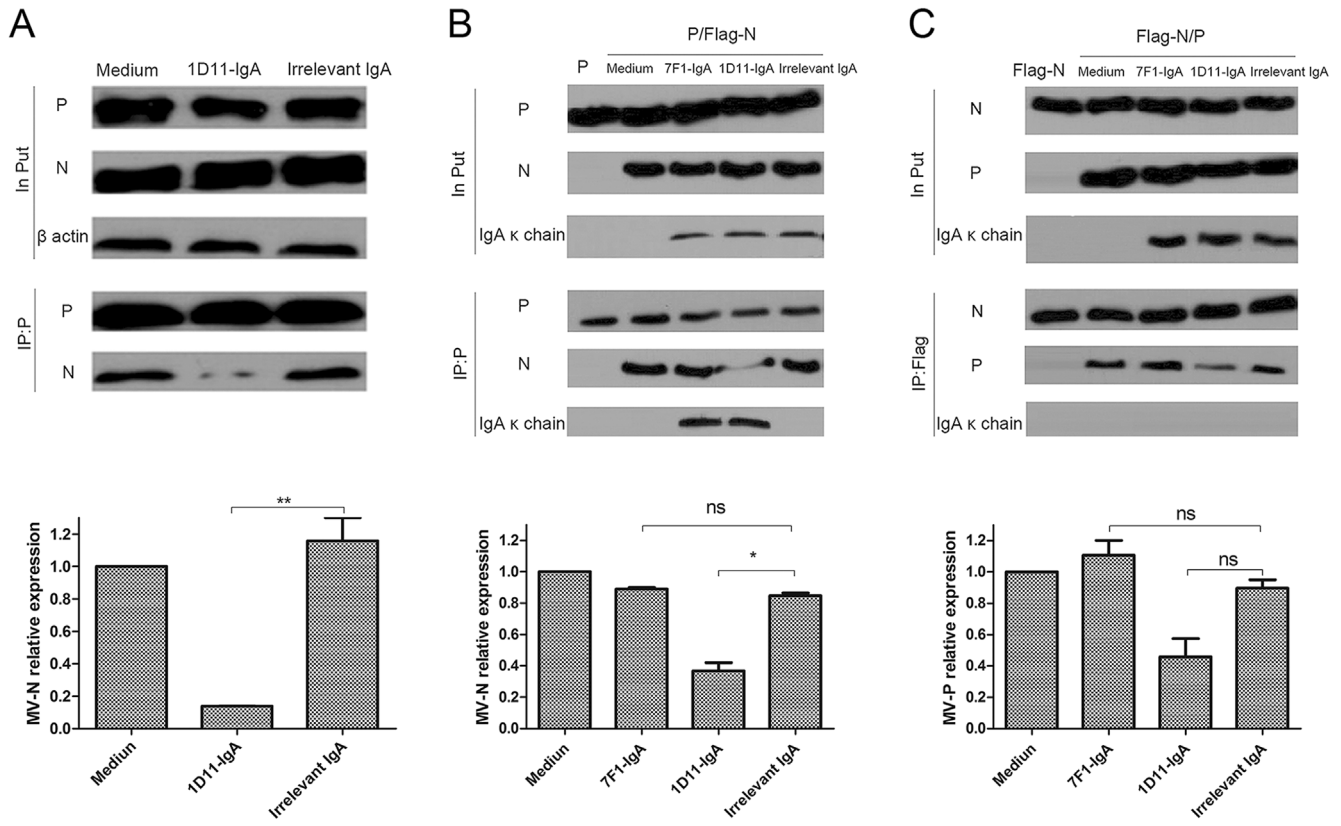

Fig. 4. Anti-P 1D11-IgA inhibits interaction of P protein with N protein in Vero-pIgR cells. (A) Vero-pIgR cells grown in transwells were infected with measles virus at an MOI of 1. Then, 24 h.p.i., 20 μg of anti-P 1D11-IgA mAb in 120 μl DMEM, 20 μg of HIV gp120 specific mAb as an irrelevant antibody control in 120 μl DMEM, or 120 μl DMEM alone was added to the basal chambers. 30 h after initial exposure to the virus, cell lysates were collected and a P specific IgG (anti-P 8C4-IgG) antibody was used to co-immunoprecipitate the complex. The complex was analyzed by western blotting to detect P and N proteins. The graph represents the intensity of N protein expression in experiment group over N protein expression in the control condition (medium alone). **(B)** and **(C)** Vero-pIgR cells were co-transfected with plasmids encoding P and Flag-N, respectively, and at the same time 20 μg of anti-P 7F1-IgA, 1D11-IgA, or anti-HIV gp120 IgA as irrelevant control in 120 μl DMEM, or 120 μl DMEM alone as negative control were added to the basal chambers. 48 h after transfection, cell lysates were collected, a P specific IgG (8C4-IgG) was used to co-immunoprecipitate the complex including P protein **(B)** and anti-Flag antibody was used to co-immunoprecipitate the complex including N protein **(C)**. Complexes were analyzed via western blotting to detected N protein (by anti-N 16CF7-IgG), P protein (by anti-P 7G4-IgG) and IgA (by anti-IgA κ chain antibody). The graph represents the intensity of P or N protein expression in experiment group over P or N protein expression in the control condition (medium alone). Error bars, mean ± SD of two independent experiments. ns, $p \geq 0.05$, *, $p < 0.05$, **, $p < 0.01$.

phosphoprotein-specific IgA antibody can interrupt the formation of P-N complex inside the epithelial cell. Although the effect of 1D11-IgA on viral replication was modest, our study provides experimental evidence that the P is a potential therapeutic antiviral target. Due to its interactive activities of P with multiple viral and cellular partners, more potential therapeutic targets on P might be approached. For instance, the P_{XD} in the C-terminal moiety of P protein (PCT) can interact with N_{TAIL} of N (P_{XD}-N_{TAIL}), which induces the folding of the α-MORE of the N_{TAIL} (Johansson et al., 2003) and is fundamental for recruiting the P-L complex to the nucleocapsid (Longhi, 2009). Targeting on this N-binding site of P (P_{XD}) might also compromise the N-P complex and interfere with viral replication. However, the presence of a secondary N-binding site in P (P_{XD}) and the homo-tetrameric nature of P which adds high avidity to P-N interactions may undermine the impact of targeting any of these interfaces in isolation. The mechanism of disorder-to-order transition of the MoRE is also poorly understood and may compromise stable binding of an inhibitor. Therefore, further studies are needed for evaluating potential therapeutics targeting N-P interfaces. In particular, the interactive activities of P with multiple cellular partners endow P with more potential for searching novel druggable sites on the interface between P and cellular factors. Indeed, we have recently found that an IgA antibody 7F1-IgA which targets the interface between P and a cellular factor inhibits MV replication through a mechanism different from that of 1D11-IgA (unpublished data).

In summary, our results provide valuable information for the drug-seeking community in search of novel druggable sites in the mononegavirales polymerase complex. The study serves as a proof-of-concept assessment of the druggability of mononegavirales N-P interfaces that should inform analogous approaches against other paramyxoviruses and, for instance, related pneumoviruses and filoviruses.

Author contributions

D.Z., Y.Y., B.Z., J.Y., Y.C., H.Y., W.Z., L. C., F.C., X.L., E.Z., J.Yang, and M.Z. performed experiments and analyzed data. Huimin.Yan., L.D., Q.H. and M.C. designed the study and wrote the manuscript.

Disclosure

The authors declare no potential conflicts of interest with respect to the authorship and/or publication of this article.

Acknowledgements

This work was supported by grants from the National Natural Science Foundation of China (No. 31670932, 31200689, 81461130019), and the National Key R&D Program of China (No.

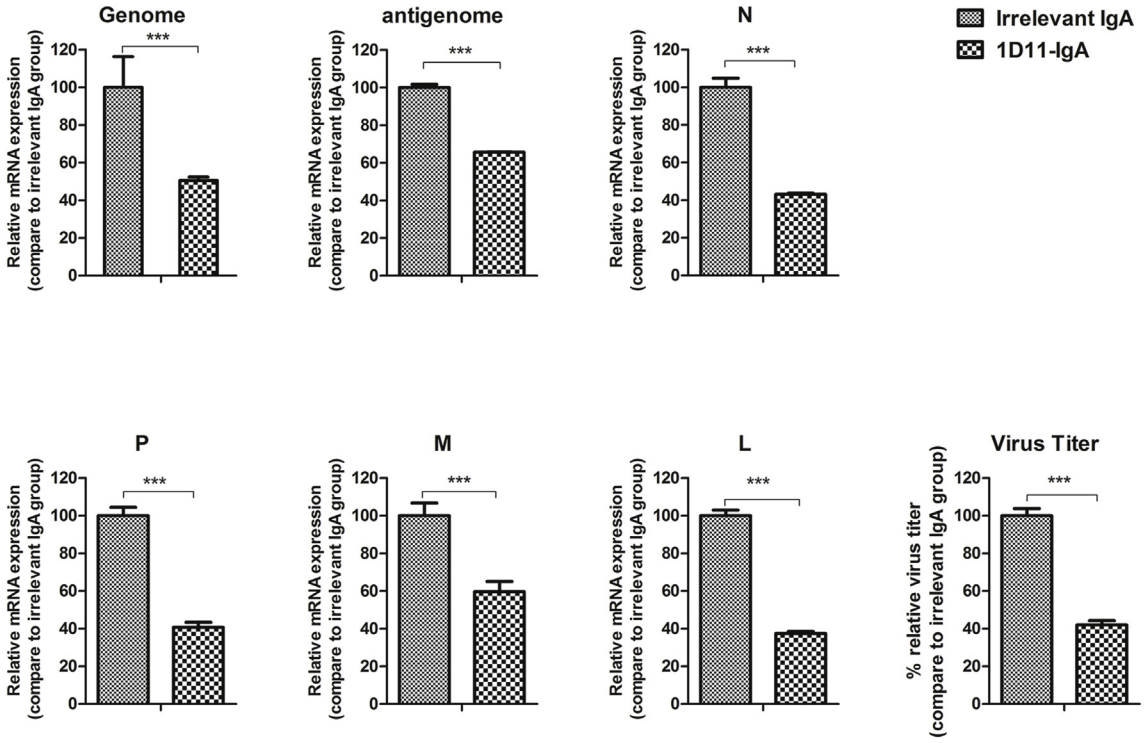

Fig. 5. Anti-P 1D11-IgA inhibits transcription and replication of MV. Vero-pIgR cells grown in transwells were infected with measles virus at an MOI of 1. Then, 2 h.p.i., 20 μg of anti-P 1D11-IgA mAb in 120 μl DMEM were added. Cell lysates were collected 48 h after initial exposure to virus, and negative-strand genome RNA, positive-strand full-length RNA and mRNA of N, P, M, L, and β-actin were assessed by RT-PCR. Virus titers were assessed by plaque assay. The percentages of RNA expression were calculated over those in irrelevant IgA control based on double delta Ct analysis with the irrelevant IgA control as 100%. **, $p < 0.01$, ***, $p < 0.001$.

2016YFC1201000). We thank Dr. Ding Gao and Dr. Hao Tang at the core facility in the Wuhan Institute of Virology for technical support.

Appendix A. Supplementary data

Supplementary data to this article can be found online at https://doi.org/10.1016/j.antiviral.2018.11.014.

References

Blocquel, D., Habchi, J., Durand, E., Sevajol, M., Ferron, F., Erales, J., Papageorgiou, N., Longhi, S., 2014. Coiled-coil deformations in crystal structures: the measles virus phosphoprotein multimerization domain as an illustrative example. Acta Crystallogr. D Biol. Crystallogr. 70, 1589–1603.

Bloyet, L.M., Brunel, J., Dosnon, M., Hamon, V., Erales, J., Gruet, A., Lazert, C., Bignon, C., Roche, P., Longhi, S., Gerlier, D., 2016. Modulation of Re-initiation of measles virus transcription at intergenic regions by P-XD to N-TAIL binding strength. PLoS Pathog. 12.

Bonetti, D., Camilloni, C., Visconti, L., Longhi, S., Brunori, M., Vendruscolo, M., Gianni, S., 2016. Identification and structural characterization of an intermediate in the folding of the measles virus X domain. J. Biol. Chem. 291, 10886–10892.

Bourhis, J.M., Canard, B., Longhi, S., 2006. Structural disorder within the replicative complex of measles virus: functional implications. Virology 344, 94–110.

Bourhis, J.M., Johansson, K., Receveur-Brechot, V., Oldfield, C.J., Dunker, K.A., Canard, B., Longhi, S., 2004. The C-terminal domain of measles virus nucleoprotein belongs to the class of intrinsically disordered proteins that fold upon binding to their physiological partner. Virus Res. 99, 157–167.

Bourhis, J.M., Receveur-Brechot, V., Oglesbee, M., Zhang, X., Buccellato, M., Darbon, H., Canard, B., Finet, S., Longhi, S., 2005. The intrinsically disordered C-terminal domain of the measles virus nucleoprotein interacts with the C-terminal domain of the phosphoprotein via two distinct sites and remains predominantly unfolded. Protein Sci. Publ. Protein Soc. 14, 1975–1992.

Brunel, J., Chopy, D., Dosnon, M., Bloyet, L.M., Devaux, P., Urzua, E., Cattaneo, R., Longhi, S., Gerlier, D., 2014. Sequence of events in measles virus replication: role of phosphoprotein-nucleocapsid interactions. J. Virol. 88, 10851–10863.

Buchholz, C.J., Retzler, C., Homann, H.E., Neubert, W.J., 1994. The carboxy-terminal domain of sendai virus nucleocapsid protein is involved in complex-formation between phosphoprotein and nucleocapsid-like particles. Virology 204, 770–776.

Burns, J.W., SiadatPajouh, M., Krishnaney, A.A., Greenberg, H.B., 1996. Protective effect of rotavirus VP6-specific IgA monoclonal antibodies that lack neutralizing activity. Science 272, 104–107.

Cevik, B., Holmes, D.E., Vrotsos, E., Feller, J.A., Smallwood, S., Moyer, S.A., 2004. The phosphoprotein (P) and L binding sites reside in the N-terminus of the L subunit of the measles virus RNA polymerase. Virology 327, 297–306.

Corthesy, B., 2013. Multi-faceted functions of secretory IgA at mucosal surfaces. Front. Immunol. 4.

Corthesy, B., Benureau, Y., Perrier, C., Fourgeux, C., Parez, N., Greenberg, H., Schwartz-Cornil, I., 2006. Rotavirus anti-VP6 secretory immunoglobulin a contributes to protection via intracellular neutralization but not via immune exclusion. J. Virol. 80, 10692–10699.

Curran, J., Marq, J.B., Kolakofsky, D., 1995. An N-terminal domain of the Sendai paramyxovirus P protein acts as a chaperone for the NP protein during the nascent chain assembly step of genome replication. J. Virol. 69, 849–855.

Devasthanam, A.S., 2014. Mechanisms underlying the inhibition of interferon signaling by viruses. Virulence 5, 270–277.

Dosnon, M., Bonetti, D., Morrone, A., Erales, J., di Silvio, E., Longhi, S., Gianni, S., 2015. Demonstration of a folding after binding mechanism in the recognition between the measles virus N-TAIL and X domains. ACS Chem. Biol. 10, 795–802.

Erales, J., Blocquel, D., Habchi, J., Beltrandi, M., Gruet, A., Dosnon, M., Bignon, C., Longhi, S., 2015. Order and disorder in the replicative complex of paramyxoviruses. Adv. Exp. Med. Biol. 870, 351–381.

Gruet, A., Dosnon, M., Blocquel, D., Brunel, J., Gerlier, D., Das, R.K., Bonetti, D., Gianni, S., Fuxreiter, M., Longhi, S., Bignon, C., 2016. Fuzzy regions in an intrinsically disordered protein impair protein-protein interactions. FEBS J. 283, 576–594.

Guryanov, S.G., Liljeroos, L., Kasaragod, P., Kajander, T., Butcher, S.J., 2015. Crystal structure of the measles virus nucleoprotein core in complex with an N-terminal region of phosphoprotein. J. Virol. 90, 2849–2857.

Huang, Y.T., Miller, C.J., Wong, V., Fujioka, H., Nedrud, J.G., Lamm, M.E., 1999. Replication and budding of simian immunodeficiency virus in polarized epithelial cells. Virology 257, 24–34.

Huber, M., Cattaneo, R., Spielhofer, P., Orvell, C., Norrby, E., Messerli, M., Perriard, J.C., Billeter, M.A., 1991. Measles-virus phosphoprotein retains the nucleocapsid protein in the cytoplasm. Virology 185, 299–308.

Johansson, K., Bourhis, J.M., Campanacci, V., Cambillau, C., Canard, B., Longhi, S., 2003. Crystal structure of the measles virus phosphoprotein domain responsible for the induced folding of the C-terminal domain of the nucleoprotein. J. Biol. Chem. 278, 44567–44573.

Karlin, D., Ferron, F.O., Canard, B., Longhi, S., 2003. Structural disorder and modular organization in Paramyxovirinae N and P. J. Gen. Virol. 84, 3239–3252.

Karlin, D., Longhi, S., Receveur, V., Canard, B., 2002. The N-terminal domain of the phosphoprotein of Morbilliviruses belongs to the natively unfolded class of proteins. Virology 296, 251–262.

Kingston, R.L., Hamel, D.J., Gay, L.S., Dahlquist, F.W., Matthews, B.W., 2004. Structural

basis for the attachment of a paramyxoviral polymerase to its template. Proc. Natl. Acad. Sci. U. S. A. 101, 8301–8306.
Kirchdoerfer, R.N., Abelson, D.M., Li, S., Wood, M.R., Saphire, E.O., 2015. Assembly of the ebola virus nucleoprotein from a chaperoned VP35 complex. Cell Rep. 12, 140–149.
Kohler, G., Milstein, C., 1975. Continuous cultures of fused cells secreting antibody of predefined specificity. Nature 256, 495–497.
Lamm, M.E., 1997. Interaction of antigens and antibodies at mucosal surfaces. Annu. Rev. Microbiol. 51, 311–340.
Longhi, S., 2009. Nucleocapsid structure and function. Curr. Top Microbiol. 329, 103–128.
Longhi, S., Receveur-Brechot, V., Karlin, D., Johansson, K., Darbon, H., Bhella, D., Yeo, R., Finet, S., Canard, B., 2003. The C-terminal domain of the measles virus nucleoprotein is intrinsically disordered and folds upon binding to the C-terminal moiety of the phosphoprotein. J. Biol. Chem. 278, 18638–18648.
Lycke, N.Y., Bemark, M., 2017. The regulation of gut mucosal IgA B-cell responses: recent developments. Mucosal Immunol. 10, 1361–1374.
Mantis, N.J., Rol, N., Corthesy, B., 2011. Secretory IgA's complex roles in immunity and mucosal homeostasis in the gut. Mucosal Immunol. 4, 603–611.
Mazanec, M.B., Kaetzel, C.S., Lamm, M.E., Fletcher, D., Nedrud, J.G., 1992. Intracellular neutralization of virus by immunoglobulin A antibodies. Proc. Natl. Acad. Sci. U. S. A. 89, 6901–6905.
Mazanec, M.B., Kaetzel, C.S., Lamm, M.E., Fletcher, D., Peterra, J., Nedrud, J.G., 1995. Intracellular neutralization of Sendai and influenza viruses by IgA monoclonal antibodies. Adv. Exp. Med. Biol. 371A, 651–654.
Mazanec, M.B., Nedrud, J.G., Kaetzel, C.S., Lamm, M.E., 1993. A three-tiered view of the role of IgA in mucosal defense. Immunol. today 14, 430–435.
Noton, S.L., Fearns, R., 2015. Initiation and regulation of paramyxovirus transcription and replication. Virology 479–480, 545–554.
Ryan, K.W., Portner, A., 1990. Separate domains of sendai virus-P protein are required for binding to viral nucleocapsids. Virology 174, 515–521.
Spehner, D., Drillien, R., Howley, P.M., 1997. The assembly of the measles virus nucleoprotein into nucleocapsid-like particles is modulated by the phosphoprotein. Virology 232, 260–268.
Strugnell, R.A., Wijburg, O.L., 2010. The role of secretory antibodies in infection immunity. Nat. Rev. Microbiol. 8, 656–667.
Yan, H., Lamm, M.E., Bjorling, E., Huang, Y.T., 2002. Multiple functions of immunoglobulin A in mucosal defense against viruses: an in vitro measles virus model. J. Virol. 76, 10972–10979.
Zhou, D., Zhang, Y., Li, Q., Chen, Y., He, B., Yang, J., Tu, H., Lei, L., Yan, H., 2011. Matrix protein-specific IgA antibody inhibits measles virus replication by intracellular neutralization. J. Virol. 85, 11090–11097.